Journal of Nanotechnology and Innovative Materials

Research Article

A Purely Dissipative Third-Order Exceptional Point in a Plasmonic Nanocavity with Two Quantum Dots: Exact Conditions and the Absence of an Enhanced Observable Response

Narmin A. Azizli

Department of Mechanics and Mathematics, School of Advanced Technologies and Innovation Engineering, Western Caspian University, 17A, Ahmad Rajabli Street, III Parallel, AZ1072 Baku, Azerbaijan

Received: 27.06.2026 Accepted: 26.07.2026 Published: 31.07.2026

https://doi.org/10.54414/WSLM7544

Abstract

Third-order exceptional points in cavity systems have so far been obtained by introducing optical or mechanical gain, which restricts them to platforms where gain can be engineered. We show that two semiconductor quantum dots in a lossy plasmonic nanocavity host such a point with loss alone, and we solve the coalescence problem for the 3 × 3 effective Hamiltonian in closed form. The conditions leave no free parameter: the cavity sits at the mean transition frequency of the dots, the direct dipole-dipole coupling vanishes, the loss contrast obeys $\kappa - \gamma = 3\sqrt{3}g$, and the two dots are detuned from each other by exactly one coupling constant, $\omega_1 - \omega_2 = g$. The tuning knob is the detuning between the emitters rather than a gain rate. We confirm that the effective Hamiltonian becomes a single Jordan block of size three and that the coalescence also appears in the spectrum of the full Liouvillian, where three eigenvalues agree to one part in 10^5 of the linewidth, and the geometric multiplicity remains one, so quantum jumps do not remove it. The eigenvalue splitting follows $(\varepsilon g^2)^{(1/3)}$ for a cavity perturbation ε, and measured against the linewidth it exceeds the second-order response of the same device by a factor of 4 to 12 over four decades. The steady-state cavity population, however, responds linearly in ε with a fitted exponent of 1.000 and an advantage over the second-order point of only 1.09. The reason is structural: the characteristic polynomial depends on ε linearly at fixed frequency, so the resolvent stays analytic even though the pole positions do not. The cube-root law therefore describes where the poles sit and not what a spectroscopic measurement returns. We also find that a residual dipole-dipole coupling of 10^{-3} g restores linear eigenvalue response, which sets a minimum interdot separation of 12 to 36 nm and conflicts with the tight confinement that produces large coupling in plasmonic gaps.

Keywords: non-Hermitian physics, third-order exceptional point, Liouvillian spectrum, coupled quantum dots, plasmonic nanocavity, Lindblad master equation

1. Introduction

An exceptional point is a parameter value at which several eigenvalues of a non-Hermitian operator become equal, and their eigenvectors coalesce simultaneously [1]. The operator is then defective, and the spectral response to a perturbation ε loses its analyticity: for a coalescence of order n, the eigenvalues separate as $\varepsilon^{(1/n)}$. Optical and photonic systems have been the main testing ground, and the general theory is reviewed by Miri and Alù [2] and by Özdemir and co-workers [3].

Third-order points attract attention because the exponent 1/3 promises a larger response than the square root of a second-order point. They were first reached in coupled microring resonators with balanced gain and loss [4], and third-order exceptional points have also been investigated in layered optical microdisk cavities [5]. Proposals for quantum platforms followed. Almost all of them share a requirement. The pseudo-Hermitian condition used by Xiong and co-workers for a three-mode optomechanical system needs one resonator with gain [6], [7], the superconducting-circuit realisation of an exceptional surface uses balanced gain and loss [8], and the ion-cavity scheme of Kim and co-workers relies on an engineered pumping configuration [9]. Gain is not available in every platform, and in plasmonic nanostructures it is particularly awkward.

This paper starts from a system in which there is no gain at all. Two semiconductor quantum dots sit in a single-mode plasmonic nanocavity, each coupled to the cavity with strength g, with a possible direct dipole-dipole term J between them. Room-temperature strong coupling between single emitters and plasmonic gap modes is established experimentally [10], [11], with couplings of tens of meV against cavity linewidths of a hundred meV or more, and the broader physics of strong coupling between surface plasmon polaritons and quantum emitters has been reviewed extensively [12]. In the single-excitation sector, this is a three-level non-Hermitian problem, the smallest that can support a third-order coalescence, and every diagonal imaginary part is a loss.

We answer two questions. The first is whether the coalescence exists at all in such a system and under what conditions, and the answer is a single isolated point with a closed form in which the detuning between the two dots plays the role that a gain rate plays elsewhere. The second question is what the coalescence is worth. Here our result is negative, and we consider it the more useful of the two. The cube-root law governs the positions of the poles, but the steady-state optical response of the device is linear in ε, with essentially no advantage over a second-order point. This is a concrete instance of the general warning raised by Langbein [13] and by Lau and Clerk [14], worked out for a specific system rather than in the abstract.

2. Model

2.1. Hamiltonian and Master Equation

Two quantum dots with transition frequencies ω_1 and ω_2 couple to a cavity mode of frequency ω_c. In the rotating wave approximation, and with ħ = 1, the Hamiltonian in a frame rotating at the drive frequency ω_L reads

$$H = \Delta_c a^\dagger a + \Delta_1 \sigma_1^+ \sigma_1^- + \Delta_2 \sigma_2^+ \sigma_2^- + g\left(a^\dagger \sigma_1^- + a\sigma_1^+\right) + g\left(a^\dagger \sigma_2^- + a\sigma_2^+\right) + J(\sigma_1^+ \sigma_2^- + \sigma_2^+ \sigma_1^-) + E\left(a + a^\dagger\right) \quad (1)$$

where $\Delta_c = \omega_c - \omega_L$ and $\Delta_i = \omega_i - \omega_L$ are the detunings, a is the cavity annihilation operator, $\sigma_i^\pm$ are the raising and lowering operators of dot i, J is the direct dipole-dipole coupling, and E is the amplitude of a weak coherent drive. Dissipation is treated with the Markovian master equation [15]

$$\frac{d\rho}{dt} = -i[H, \rho] + \kappa \mathcal{D}[a]\rho + \gamma \mathcal{D}[\sigma_1^-]\rho + \gamma \mathcal{D}[\sigma_2^-]\rho \quad (2)$$

with the dissipator

$$\mathcal{D}[A]\rho = A\rho A^\dagger - \frac{1}{2}\left\{A^\dagger A, \rho\right\} \quad (3)$$

Here κ is the cavity photon loss, dominated by ohmic absorption in the metal, and γ is the spontaneous emission rate of each dot into modes other than the cavity. Both rates are positive. No gain enters anywhere.

2.2. Effective Non-Hermitian Hamiltonian

Set E = 0 and restrict the dynamics to the single-excitation subspace spanned by |1, g, g⟩, |0, e, g⟩ and |0, g, e⟩. Between quantum jumps, the state evolves under

$$H_{eff} = \begin{bmatrix} \omega_c - i\frac{\kappa}{2} & g & g \\ g & \omega_1 - i\frac{\gamma}{2} & J \\ g & J & \omega_2 - i\frac{\gamma}{2} \end{bmatrix} \quad (4)$$

Introducing

$$\omega_{1,2} = \omega_0 \pm \delta, \quad A = \Delta_c - iq, \quad q = \frac{\kappa - \gamma}{2}, \quad \Delta_c = \omega_c - \omega_0 \tag{5}$$

and subtracting $\omega_0 - i\gamma/2$ from the diagonal, the shifted matrix becomes

$$H' = \begin{bmatrix} A & g & g \\ g & \delta & J \\ g & J & -\delta \end{bmatrix} \tag{6}$$

The whole of the non-Hermiticity now sits in the single complex number A while every other entry is real, which is what makes the problem solvable by hand.

3. Exact Conditions for the Coalescence

The characteristic polynomial of H′ is $\lambda^3 + c_2\lambda^2 + c_1\lambda + c_0$ with

$$c_2 = -A, \quad c_1 = -(2g^2 + \delta^2 + J^2), \quad c_0 = A(\delta^2 + J^2) - 2g^2 J \tag{7}$$

A triple root requires the polynomial to equal $(\lambda - \lambda_0)^3$ with $\lambda_0 = -c_2/3 = A/3$, which gives the two complex conditions $c_1 = c_2^2/3$ and $c_0 = c_2^3/27$. The first reads

$$A^2 = -3S, \quad S = 2g^2 + \delta^2 + J^2 \tag{8}$$

S is real and positive, so A must be purely imaginary. The cavity therefore has to be tuned to the mean transition frequency of the dots, $\Delta_c = 0$, and writing $A = -iq$, the condition becomes $q^2 = 3S$. Substituting into the second condition and separating real from imaginary parts gives

$$2g^2 J = 0, \qquad \delta^2 + J^2 = \frac{q^2}{27} \tag{9}$$

The first of these forces J = 0, which is the least expected feature of the result. The coalescence survives only when the two dots have no direct coupling to each other, and any residual dipole-dipole interaction removes it. With J = 0 the remaining relations close and give $q^2 = 27g^2/4$ and $\delta^2 = g^2/4$, so the third-order point occurs at

$$\Delta_c = 0, \quad J = 0, \quad \kappa - \gamma = 3\sqrt{3}\, g, \quad \omega_1 - \omega_2 = 2\delta = g \tag{10}$$

with the threefold eigenvalue

$$\lambda_0 = \omega_0 - i\left(\frac{\gamma}{2} + \frac{\sqrt{3}\, g}{2}\right) \tag{11}$$

Every parameter is fixed once g is chosen, and the only remaining freedom is the overall energy scale. Two features are worth stating plainly. The loss contrast has to be about 5.2 times the coupling strength, which is a regime plasmonic cavities reach naturally. The two dots have to be detuned by exactly one coupling constant, so the emitters are neither degenerate nor far apart, and this detuning is the parameter that replaces the gain rate of earlier proposals [6], [7], [8], [9].

We verified equation (10) numerically for g = 30 meV. The three eigenvalues agree with λ_0 to 3×10^{-4} meV, which is the accuracy any eigenvalue routine can reach near a defective matrix since the error scales as the cube root of the machine epsilon. The matrix $H' - \lambda_0 I$ has rank two, so only one eigenvector survives, and $(H' - \lambda_0 I)^3$ vanishes to 1.9×10^{-11} in the Frobenius norm. The Jordan form is a single block of size three. Figure 1 sweeps the dot-dot detuning at fixed loss contrast, and the real and imaginary parts of all three branches meet at $\delta = g/2$.

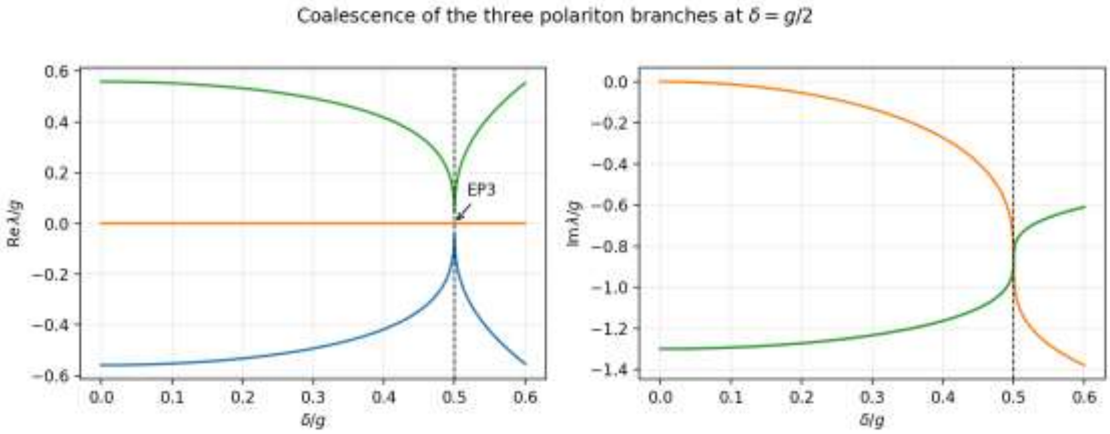

Figure 1. Real and imaginary parts of the three eigenvalues of H′ against the dot-dot detuning δ, at Δ_c = 0, J = 0, and κ − γ = 3√3g. The three branches meet at δ = g/2.

Figure 2 maps the discriminant of the characteristic polynomial over the plane of δ and loss contrast. The dark curves are second-order exceptional lines, and they meet in a cusp at the point of equation (10).

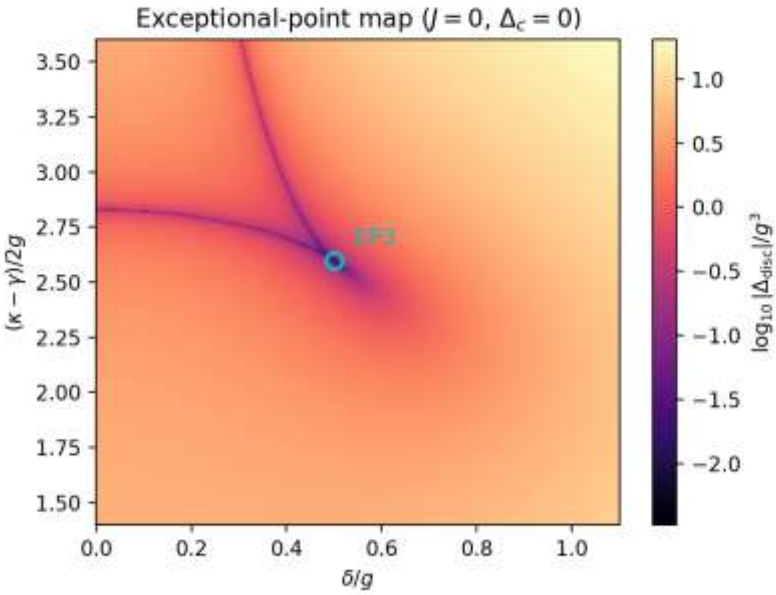

Figure 2. Logarithm of the discriminant of the characteristic polynomial in the (δ, κ − γ) plane for J = 0 and Δ_c = 0. The two second-order lines meet at the third-order point marked in cyan.

4. The Coalescence in the Full Liouvillian

The effective Hamiltonian of equation (4) drops the recycling term of the master equation, so a coalescence found there need not survive in the full dynamics. Exceptional points of a Liouvillian and of the corresponding non-Hermitian Hamiltonian are known to differ in general. We therefore diagonalised the Liouvillian of equation (2) directly, on a Hilbert space of dimension 3 × 2 × 2 with the cavity truncated at three photons.

The single-excitation coherences of the density matrix appear in the Liouvillian spectrum at $\mu = -i\lambda$, where λ are the eigenvalues of H_eff. At the parameters of equation (10), the three Liouvillian eigenvalues closest to that prediction lie within 5.6×10^{-4} meV of each other, which is 1.1×10^{-5} of the coalescence linewidth. The matrix $\mathscr{L} - \mu I$ has only one vanishing singular value at that eigenvalue, so its geometric multiplicity is one, and the Liouvillian is defective there as well. Quantum jumps shift the coalescence by an amount far below any linewidth and do not destroy it. This is the first of the two checks that a reader would reasonably demand.

5. Eigenvalue Response and its Resolvability

An analyte binding to the metal surface changes the local permittivity by δε_r and shifts the cavity frequency by

$$\varepsilon = \frac{\omega_c \, \delta\varepsilon_r}{2{n_0}^2} \qquad (12)$$

which perturbs the (1,1) element of H′ alone. Expanding the characteristic polynomial about the coalescence with the cofactor of that element gives

$$(\lambda - \lambda_0)^3 = \varepsilon\left({\lambda_0}^2 - \delta^2\right) = -\varepsilon g^2 \qquad (13)$$

since $\lambda_0 = -i\sqrt{3}g/2$ and $\delta = g/2$ in the shifted frame. The roots therefore separate as

$$|\lambda - \lambda_0| = (\varepsilon g^2)^{\frac{1}{3}}, \quad |\Delta\lambda_{max}| = \sqrt{3}(\varepsilon g^2)^{\frac{1}{3}} \qquad (14)$$

with the three branches spaced by 120 degrees in the complex plane. Figure 3 compares this with the second-order point of the same device, reached by making the dots degenerate so that the dark state decouples and the cavity couples to the bright state with √2g [16]. That configuration has its exceptional point at κ − γ = 4√2g and responds as the square root of ε. Table 1 lists the numbers.

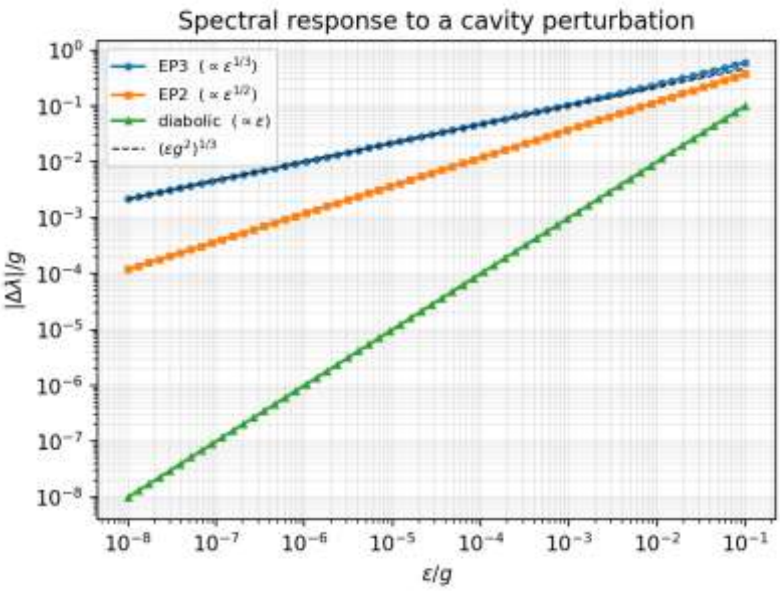

Figure 3. Eigenvalue splitting against the cavity perturbation ε on logarithmic axes. The slopes are 1/3, 1/2, and 1. The dashed line is equation (14).

Table 1. Eigenvalue splitting for the three cases of Figure 3.

ε / g	EP3, |δλ| / g	EP2, |δλ| / g	Conventional, |δω| / g	EP3 / EP2
10^{-2}	2.409×10^{-1}	1.189×10^{-1}	10^{-2}	2.03
10^{-3}	1.052×10^{-1}	3.761×10^{-2}	10^{-3}	2.80
10^{-4}	4.751×10^{-2}	1.189×10^{-2}	10^{-4}	4.00
10^{-5}	2.178×10^{-2}	3.761×10^{-3}	10^{-5}	5.79
10^{-6}	1.005×10^{-2}	1.189×10^{-3}	10^{-6}	8.45

A splitting is only meaningful next to a linewidth, and the three cases have very different linewidths. At the third-order point the coalesced triple has a full width of √3g, at the second-order point the width is 2√2g, and a conventional measurement on the same platform works against the bare cavity width κ. Normalising each splitting by its own width gives

$$R_3 = \left(\frac{\varepsilon}{g}\right)^{\frac{1}{3}}, \qquad R_2 = 0.841 \left(\frac{\varepsilon}{g}\right)^{\frac{1}{2}} \tag{15}$$

So the advantage of the third-order point survives the normalisation and in fact grows, because its linewidth is the narrowest of the three. Table 2 and Figure 4 give the numbers. Against the second-order point of the same device, the gain runs from 2.8 at $\varepsilon = 10^{-2}$ g to 12 at $\varepsilon = 10^{-6}$ g. Against a conventional shift measurement in the same cavity, it is five orders of magnitude. The splitting reaches ten percent of the linewidth at $\varepsilon = 0.026$ meV for g = 30 meV, which is a spectroscopically plausible target.

Table 2. Splitting normalised by the corresponding linewidth.

ε / g	EP3, split / FWHM	EP2, split / FWHM	Conventional, shift / FWHM	EP3 / EP2
10^{-2}	2.390×10^{-1}	8.409×10^{-2}	1.924×10^{-3}	2.84
10^{-3}	1.050×10^{-1}	2.659×10^{-2}	1.924×10^{-4}	3.95
10^{-4}	4.750×10^{-2}	8.409×10^{-3}	1.924×10^{-5}	5.65
10^{-5}	2.178×10^{-2}	2.659×10^{-3}	1.924×10^{-6}	8.19
10^{-6}	1.005×10^{-2}	8.409×10^{-4}	1.924×10^{-7}	11.95

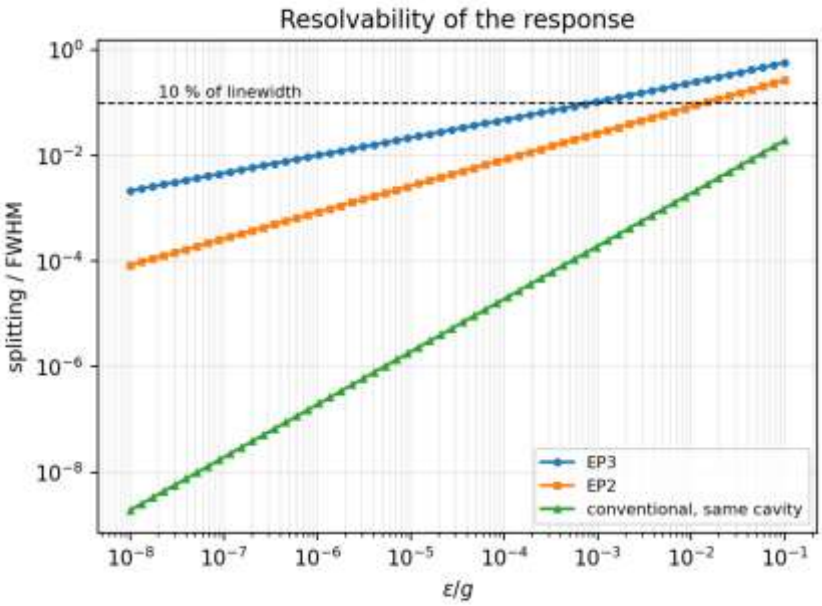

Figure 4. Splitting divided by the full width at half maximum of the relevant resonance, for the third-order point, the second-order point, and a conventional shift measurement in the same cavity.

6. Response of a Measurable Quantity

Everything in section 5 concerns eigenvalues, which are not what a spectrometer records. To find the response of an observable, we solved the master equation for the steady state under a weak coherent drive, $\mathscr{L}\rho\_ss = 0$, by direct linear inversion with the trace condition substituted for one row. The mean cavity population changes by less than 2×10^{-5} in relative terms between Fock cutoffs of three and five, so the truncation is converged at the drive amplitude used, E = 0.02 g.

Figure 5 shows the steady-state cavity population against drive detuning for three values of the cavity loss. Below the exceptional value, the spectrum has three resolved polariton peaks. At κ = κ_EP they merge into a single line, and above it the response is one broad peak.

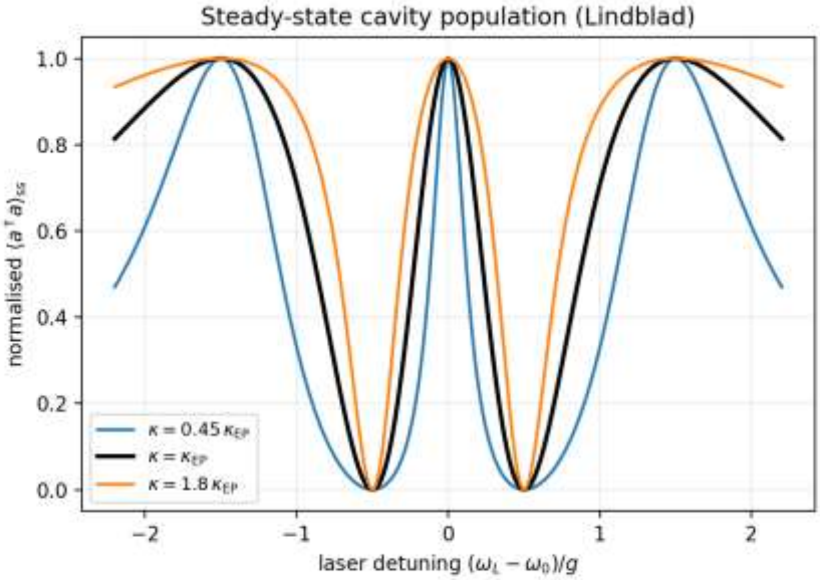

Figure 5. Normalised steady-state cavity population against laser detuning for three cavity loss rates.

We then applied the perturbation ε and measured how much the spectrum changes, taking the largest absolute change in the population normalised by its peak value. The result is Figure 6 and Table 3. Over more than two decades, the response follows a power law with a fitted exponent of 1.000, both at the third-order point and at the second-order point, and the ratio between the two is 1.09 and independent of ε. The cube-root behaviour is absent from the observable.

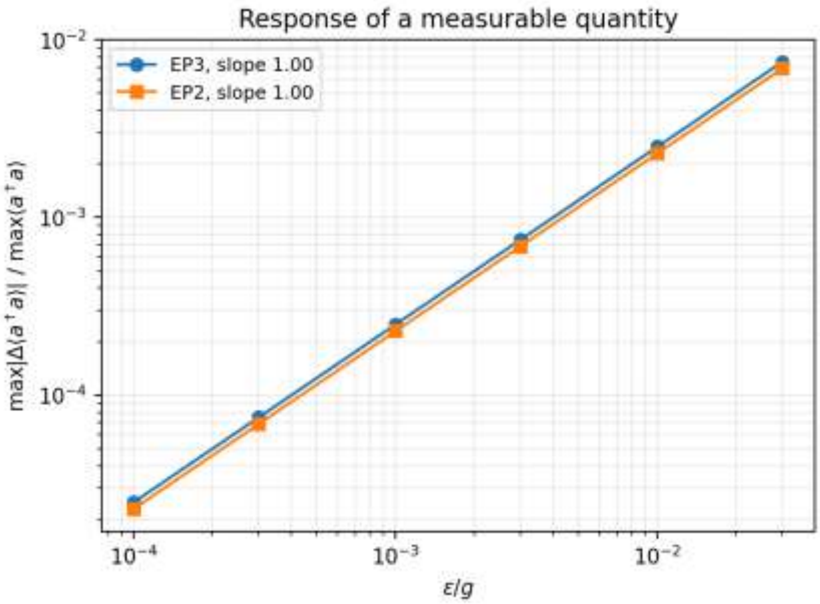

Figure 6. Relative change of the steady-state cavity population under a perturbation ε, at the third-order point and at the second-order point. Both are linear in ε.

Table 3. Response of the steady-state cavity population.

ε / g	EP3, max|Δ⟨n⟩| / ⟨n⟩max	EP2, max|Δ⟨n⟩| / ⟨n⟩max	EP3 / EP2
10^{-4}	2.498×10^{-5}	2.296×10^{-5}	1.09
10^{-3}	2.498×10^{-4}	2.296×10^{-4}	1.09
10^{-2}	2.499×10^{-3}	2.296×10^{-3}	1.09

The reason is structural rather than numerical, and it can be read off the characteristic polynomial. With the perturbation included,

$$P(\omega) = (\omega - \lambda_0)^3 - \varepsilon(\omega^2 - \delta^2), \qquad \frac{\partial P(\omega)}{\partial \varepsilon} = -(\omega^2 - \delta^2) \tag{16}$$

At a fixed observation frequency ω, the polynomial depends on ε linearly, and every steady-state response of the driven system is built from the resolvent, whose denominator is P(ω). The lineshape therefore changes at first order in ε. The cube root enters only when one asks where the roots of P have moved, and at a third-order point those three roots sit inside a single linewidth with residues that very nearly cancel, so no spectroscopic measurement separates them. Individual eigenvalues are not observables of the driven steady state.

This does not contradict section 5. It says that the normalised splitting of Figure 4 is the right figure of merit only for an experiment that can resolve the poles individually, for instance a time-domain measurement of the ringdown or a scheme that isolates one eigenvector. For the ordinary transmission or scattering measurement that an exceptional-point sensor is usually imagined to perform, the enhancement is not there. Langbein [13] and Lau and Clerk [14] reached the same conclusion for second-order points from noise arguments, and Wiersig [17] reviews the cases where an enhancement does survive. What the present calculation adds is that the obstruction appears already at the level of the deterministic response, before any noise is introduced.

7. Sensitivity to a Residual Dipole-Dipole

Because equation (9) forces J to vanish exactly, the tolerance on J is a practical question. A finite J splits the triple root into a second-order point plus a separate eigenvalue, and the residual splitting grows as the cube root of J, so it already reaches five percent of g at $J \approx 1.1 \times 10^{-3}$ g. At that value, the local response exponent measured at $\varepsilon = 10^{-5}$ g has returned to 0.99. Figure 7 shows both curves.

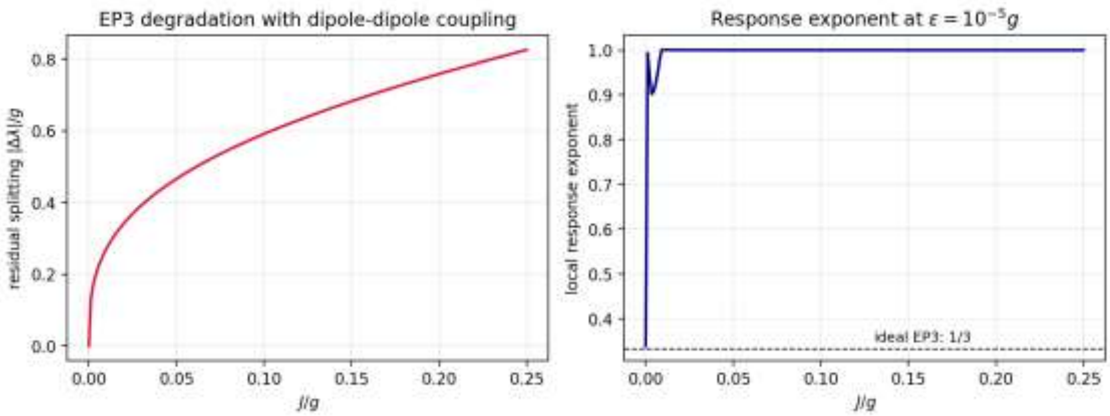

Figure 7. Left: residual eigenvalue splitting at the nominal exceptional point against the dipole-dipole coupling J. Right: local response exponent at $\varepsilon = 10^{-5}$ g, with the ideal value 1/3 marked.

For g = 30 meV, the tolerance is $|J| \lesssim 0.03$ meV. Treating the interaction as a point dipole coupling,

$$J = \frac{\mu^2}{4\pi\varepsilon_0 r^3} \tag{17}$$

this gives a minimum separation of about 12 nm for a transition dipole of 10 D, 20 nm for 20 D, and 26 nm for 30 D. The requirement pulls against the geometry that produces a large g, because plasmonic gap modes concentrate their field over a few nanometres. A device of this kind needs a cavity whose field stays strong across a few tens of nanometres, such as an extended nanoparticle-on-mirror gap or a bowtie antenna with a wider feed, and it pays for the separation with a smaller coupling. This tension sets the design window more tightly than any of the spectral conditions.

8. Parameter Estimate

Take $\omega_0 = 1.5$ eV and g = 30 meV, within the range reported for single emitters in plasmonic gap modes at room temperature [10], [11]. Equation (10) then requires κ = 155.9 meV, a quality factor of about 9.6, which is ordinary for a gold nanoparticle-on-mirror cavity. The dot-dot detuning must be 30 meV, comfortably inside the inhomogeneous distribution of self-assembled dots and reachable with a quantum-confined Stark shift on one dot. With $\gamma = 5$ μeV, the condition is effectively $\kappa = 3\sqrt{3}g$. The linewidth at the coalescence is $\sqrt{3}g/2 \approx 26$ meV from equation (11). None of these numbers is unusual, and the demanding parts are the separation constraint of section 7 and holding the detuning at g.

9. Conclusion

A two-dot plasmonic cavity supports a third-order exceptional point without any gain, and the conditions for it are simple enough to write down exactly: the cavity on resonance with the mean dot frequency, no direct dipole-dipole coupling, $\kappa - \gamma = 3\sqrt{3}g$, and a dot-dot detuning of exactly g. The detuning between the emitters takes the role that a gain rate plays in the optomechanical and circuit realisations reported so far. The coalescence is not an artefact of the effective non-Hermitian description, since the full Liouvillian is defective at the same parameters to within one part in 10^5 of the linewidth.

The eigenvalue splitting follows the expected cube-root law, and normalised against the linewidth it beats the second-order point of the same device by a factor of 4 to 12. The steady-state optical response does not follow it. That response is linear in the perturbation with an advantage of 1.09 over the second-order point, because the characteristic polynomial enters the resolvent linearly in ε at fixed frequency while the cube root lives only in the pole positions, which are unresolvable inside one linewidth. Any proposal that treats the ε^(1/3) eigenvalue law as a sensing figure of merit for a driven cavity measurement should be read with this in mind.

Two directions follow. A time-domain measurement is not bound by the argument of section 6 and might recover the cube root, which would be worth calculating. The tolerance on the dipole-dipole coupling, one part in a thousand of g, is the practical obstacle, and a cavity geometry that keeps a large coupling across a few tens of nanometres would be the first thing such an experiment needs.

Appendix. Numerical methods

All calculations use numpy and scipy. Eigenvalues of the 3 × 3 effective Hamiltonian come from numpy.linalg.eigvals. Near a defective matrix, the accuracy of any eigenvalue routine scales as the cube root of the machine epsilon, which explains the 10^{-4} meV residual quoted in section 3, so the Jordan structure is confirmed instead through the rank of $H' - \lambda_0 I$ and the norm of its cube. The Liouvillian is assembled by column-stacking vectorisation,

$$\mathcal{L} = -i(H \otimes \mathbb{1} - \mathbb{1} \otimes H^T) + \Sigma_k \left[C_k \otimes C_k^* - \frac{1}{2} C_k^\dagger C_k \otimes \mathbb{1} - \frac{1}{2} \mathbb{1} \otimes \left(C_k^\dagger C_k \right)^T \right] \quad (18)$$

where the collapse operators are $\sqrt{\kappa}\, a$, $\sqrt{\gamma}\, \sigma_1^-$ and $\sqrt{\gamma}\, \sigma_2^-$. The steady state follows from replacing the first row of $\mathscr{L}$ with the vectorised identity and solving against a unit vector. Liouvillian eigenvalues come from dense diagonalisation of the 144 × 144 matrix and its defectiveness from the singular values of $\mathscr{L} - \mu I$. The scripts are supplied as supplementary material and reproduce every figure and number in the text.

Author Contributions

The author contributed to the conception, design, analysis, interpretation, and preparation of the manuscript and approved the final version.

Funding

No funding was received for this research.

Conflicts of Interest

The author declares no conflict of interest.

Acknowledgment

Not applicable.

Abbreviations

Exceptional Point (EP), Second-Order Exceptional Point (EP2), Third-Order Exceptional Point (EP3), Full Width at Half Maximum (FWHM), Half Width at Half Maximum (HWHM), Quantum Dot (QD), Rotating-Wave Approximation (RWA).

References

[1] Heiss WD. The physics of exceptional points. Journal of Physics A: Mathematical and Theoretical. 2012 Nov 9;45(44):444016. https://doi.org/10.1088/1751-8113/45/44/444016
[2] Miri MA, Alu A. Exceptional points in optics and photonics. Science. 2019 Jan 4;363(6422):eaar7709. https://doi.org/10.1126/science.aar7709
[3] Özdemir ŞK, Rotter S, Nori F, Yang L. Parity–time symmetry and exceptional points in photonics. Nature Materials. 2019 Aug;18(8):783-98. https://doi.org/10.1038/s41563-019-0304-9
[4] Hodaei H, Hassan AU, Wittek S, Garcia-Gracia H, El-Ganainy R, Christodoulides DN, Khajavikhan M. Enhanced sensitivity at higher-order exceptional points. Nature. 2017 Aug 10;548(7666):187-91. https://doi.org/10.1038/nature23280
[5] Kullig J, Yi CH, Hentschel M, Wiersig J. Exceptional points of third-order in a layered optical microdisk cavity. New Journal of Physics. 2018 Aug 1;20(8):083016. https://doi.org/10.1088/1367-2630/aad594
[6] Xiong W, Li Z, Song Y, Chen J, Zhang GQ, Wang M. Higher-order exceptional point in a pseudo-Hermitian cavity optomechanical system. Physical Review A. 2021 Dec;104(6):063508. https://doi.org/10.1103/physreva.104.063508
[7] Xiong W, Li Z, Zhang GQ, Wang M, Li HC, Luo XQ, Chen J. Higher-order exceptional point in a blue-detuned non-Hermitian cavity optomechanical system. Physical Review A. 2022 Sep;106(3):033518. https://doi.org/10.1103/physreva.106.033518
[8] Zhang G, Lin S, Feng W, Wang Y, Yu Y, Yang C. Third-order exceptional surface in a pseudo-Hermitian superconducting circuit. Science China Information Sciences. 2025 Aug;68(8):180508. https://doi.org/10.1007/s11432-025-4470-4
[9] Kim J, Ha T, Kim D, Lee D, Lee KS, Won J, Moon Y, Lee M. Third-order exceptional point in an ion–cavity system. Applied Physics Letters. 2023 Oct 16;123(16). https://doi.org/10.1063/5.0168372
[10] Chikkaraddy R, De Nijs B, Benz F, Barrow SJ, Scherman OA, Rosta E, Demetriadou A, Fox P, Hess O, Baumberg JJ. Single-molecule strong coupling at room temperature in plasmonic nanocavities. Nature. 2016 Jul 7;535(7610):127-30. https://doi.org/10.1038/nature17974
[11] Santhosh K, Bitton O, Chuntonov L, Haran G. Vacuum Rabi splitting in a plasmonic cavity at the single quantum emitter limit. Nature Communications. 2016 Jun 13;7(1):ncomms11823. https://doi.org/10.1038/ncomms11823
[12] Törmä P, Barnes WL. Strong coupling between surface plasmon polaritons and emitters: a review. Reports on Progress in Physics. 2015 Jan 1;78(1):013901. https://doi.org/10.1088/0034-4885/78/1/013901
[13] Langbein W. No exceptional precision of exceptional-point sensors. Physical Review A. 2018 Aug;98(2):023805. https://doi.org/10.1103/physreva.98.023805
[14] Lau HK, Clerk AA. Fundamental limits and non-reciprocal approaches in non-Hermitian quantum sensing. Nature Communications. 2018 Oct 17;9(1):4320. https://doi.org/10.1038/s41467-018-06477-7
[15] Breuer HP, Petruccione F. The theory of open quantum systems. OUP Oxford; 2002.
[16] Wiersig J. Enhancing the sensitivity of frequency and energy splitting detection by using exceptional points: application to microcavity sensors for single-particle detection. Physical Review Letters. 2014 May 23;112(20):203901. https://doi.org/10.1103/physrevlett.112.203901
[17] Wiersig J. Review of exceptional point-based sensors. Photonics Research. 2020 Sep 1;8(9):1457-67. https://doi.org/10.1364/prj.396115